Heliyon 10 (2024) e27601

Contents lists available at ScienceDirect

Heliyon

journal homepage: www.cell.com/heliyon

Research article

Heteroleptic (SˆC)-cyclometallated gold(III) complexes as novel antiviral agents

María Balsera-Manzanero [a], Raquel G. Soengas [b], Marta Carretero-Ledesma [a], Carlos Ratia [c], M. José Iglesias [b], Jerónimo Pachón [d,e], Fernando López-Ortiz [b,**], Elisa Cordero [a,e,f], Sara M. Soto [c,f,*], Javier Sánchez-Céspedes [a,f]

[a] *Unidad Clínica de Enfermedades Infecciosas, Microbiología y Parasitología, Instituto de Biomedicina de Sevilla (IBiS), Hospital Universitario Virgen del Rocío/CSIC/Universidad de Sevilla, Sevilla, Spain*
[b] *Área de Química Orgánica, Centro de Investigación CIAIMBITAL, Universidad de Almería, Spain*
[c] *Barcelona Institute for Global Health (ISGlobal), Universitat de Barcelona, Barcelona, Spain*
[d] *Instituto de Biomedicina de Sevilla (IBiS), Hospitales Universitarios Virgen del Rocío y Virgen Macarena/CSIC/Universidad de Sevilla, Sevilla, Spain*
[e] *Departamento de Medicina, Facultad de Medicina, Universidad de Sevilla, Sevilla, Spain*
[f] *CIBERINFEC, ISCIII, CIBER de Enfermedades Infecciosas, Instituto de Salud Carlos III, Madrid, Spain*

ARTICLE INFO

Keywords:
Adenovirus
Cycloaurated complexes
Antivirals
Metallodrugs

ABSTRACT

Despite the increasingly widespread clinical impact of adenovirus (HAdV) infections in healthy individuals and the associated high morbidity in immunosuppressed patients, particularly among the paediatric population, a specific treatment for this virus has yet to be developed. In this study, we report the anti-HAdV activity of sub-micromolar concentrations of four heteroleptic (CˆS)-cycloaurated complexes bearing a single thiophosphinamide [**Au(dpta)Cl$_2$**, **Au(dpta)(mrdtc)**, and **Au(dpta)(dedtc)**] or thiophosphonamide [**Au(bpta)(dedtc)**] chelating ligand and a dithiocarbamate moiety. In addition to their low cytotoxicity, the findings of mechanistic assays revealed that these molecules have antiviral activity by targeting stages of the viral replication cycle subsequent to DNA replication. Additionally, all four compounds showed a significant inhibition of human cytomegalovirus (HCMV) DNA replication, thereby providing evidence for potential broad-spectrum antiviral activity.

1. Introduction

Human adenovirus (HAdV) can cause life-threatening disseminated diseases in haematopoietic stem cell transplant recipients, particularly among paediatric patients; it is a well-established cause of community-acquired pneumonia in the general population [1]. Given that currently, no generally acceptable therapeutic options are available for treating HAdV infections, identifying effective new antiviral agents is imperative [2,3]. Although at present, cidofovir (CDV) is the most frequently used medication administered for the treatment of HAdV infections [4], its use tends to be limited on account of the substantial variability in its efficacy, poor bioavailability,

* Corresponding author. ISGlobal Barcelona Institute for Global Health, Campus Clínic, Hospital Clínic, Universitat de Barcelona, Rosselló, 149st floor, 08036, Barcelona, Spain.
** Corresponding author.
E-mail addresses: flortiz@ual.es (F. López-Ortiz), sara.soto@isglobal.org (S.M. Soto).

https://doi.org/10.1016/j.heliyon.2024.e27601
Received 11 August 2023; Received in revised form 1 March 2024; Accepted 4 March 2024
Available online 19 March 2024

and adverse side effects [5]. Similarly, whereas brincidofovir (BCV), a lipidic conjugate of CDV, has shown promising results in phase II and III clinical trials (NCT01231344 and NCT02087306), its use is also associated with long-term adverse effects [6,7].

Due to their diverse structural features, roles in redox processes, and multiplicity of mechanisms of action associated with metal ions, metal-based compounds have become a focus of considerable attention as viable antiviral candidates in recent years [8,9]. In particular, on account of their antimicrobial activities against viruses, bacteria, and fungi, gold (Au) complexes have attracted widespread interest across various medical fields, particularly in the infectious diseases field [10–12].

Previous studies on these complexes have predominantly centred around Au(I) complexes [13]. Auranofin [(2,3,4,6-tetra-*O*-acetyl-1-thio-β-D-glucopyranosato-κS^1)(triethylphosphoranylidene)-gold(I)], a gold-based metallodrug used for the treatment of rheumatoid arthritis, is considered the paradigm within this family of gold(I) compounds [14]. Notably, it inhibits SARS-CoV-2 replication at low micromolar concentrations [15]. Additionally, other gold(I)-derived complexes have demonstrated to have anti-leishmanial activity *in vitro* and *in vivo* at low doses [16]. Furthermore, they have demonstrated efficacy in inhibiting Chikungunya virus at different stages of the replicative cycle [17].

Compared with Au(I) complexes, the antiviral applications of their higher-oxidation-state gold(III) counterparts have been relatively little assessed. However, among those studies that have been conducted, a notable observation was made with the treatment of Chagas disease using an organometallic gold(III) complex. This complex comprises an Au(III) cation stabilized by an *S*,*N*,*S* tridentate thiosemicarbazone ligand, demonstrating the ability to eliminate the parasite without inducing cytotoxic effects on mammalian cells. Additionally, the complex contributed to a reduction in parasitaemia and tissue parasitism and exhibited protecting effects on the liver and heart *in vivo* [18]. Bis(thiosemicarbazonate)gold(III) complexes are comprised of ligands that are *S*,*N*,*N*,*S* tetracoordinated to the metal cation through two iminic nitrogen atoms and two sulphur atoms. These complexes have demonstrated anti-HIV activity by inhibiting viral infection of TZM-bl cells by 98% at a non-toxic concentration of 12.5 μM [19]. Other stable Au(III) complexes with anti-HIV activity include gold(III) dichlorides [20], tetrachlorides [21,22], and cationic porphyrin-Au(III) complexes [23]. Furthermore, in a more comprehensive study, Hewer and co-workers investigated the anti-HIV activity of a number of gold(III) complexes, including gold(III) tetrachloride, mononuclear hydroxyl, and dinuclear oxo-bridged bipyridyl chelated NˆN systems, C(4)-metalated derivatives of *N*-phenylpyrazole gold(III) dichloride, and CˆN-cyclometalated compounds. The authors found these complexes to be effective inhibitors of HIV-1 reverse transcriptase and HIV-1 integrase at low micromolar concentrations. They proposed that the strong oxidative capacities of these complexes are the most probable factor contributing to the inhibition of target proteins [22]. Recently, Ott et al. reported an extensive study on the application of metallodrugs as therapeutic agents against SARS-CoV-2 [24], in which they examined the efficacies of trihalido *N*-heterocyclic carbene (NHC) Au(III) complexes and glycoconjugates of dibromo Au (III) dithiocarbamates. Both types of complexes demonstrated good activity against the SARSCoV-2 papain-like protease PLpro, with the dithiocarbamate derivatives being among the most potent of the 105 complexes screened.

In contrast to the strong interest shown in cyclometalated and dithiocarbamate Au(III) complexes for developing anticancer agents and alternatives to cisplatin and platinum analogues [25], few studies have investigated these compounds with a goal of discovering antiviral metallodrugs [22]. In this context, cyclometallation is a particularly useful strategy for stabilizing gold ions in the +3 oxidation state [26]. Previously, we demonstrated that organometallic (CˆS)-cycloaurated complexes are hydrolytically stable under strongly acidic conditions and are unaffected by biological reductants such as ascorbate and glutathione. Moreover, when used in combination with colistin, these complexes have displayed potent antimicrobial and antibiofilm activities against a broad spectrum of antibiotic-resistant bacteria [27,28], including gram-negative strains. To the best of our knowledge, however, the antiviral activities of organometallic Au(III) complexes stabilized by C,S-chelating ligands have yet to be systematically assessed. Consequently, our objective in this study, was to evaluate the anti-HAdV properties of four (CˆS)-cycloaurated complexes bearing *ortho*-deprotonated thiophosphinamide [**Au(dpta)Cl$_2$**, **Au(dpta)(mrdtc)**, **Au(dpta)(dedtc)**] or thiophosphonamide [**Au(bpta)(dedtc)**] as the main ligands, together with a dithiocarbamate moiety (Fig. 1).

2. Methods

2.1. Cells and viruses

Human A549 (ATCC CCL-185) and HFF (ATCC SCRC-1041) cell lines and wild-type HAdV5 and HCMV (AD169) were purchased from the American Type Culture Collection (ATCC, Manassas, VA, USA). A 293β5 stable cell line overexpressing the human β5 integrin

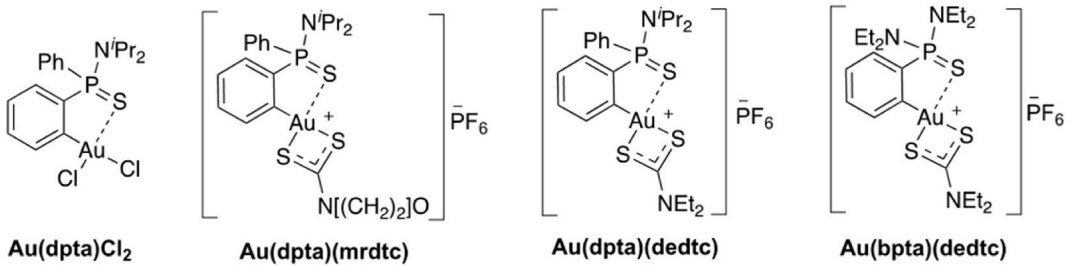

Fig. 1. Chemical structure of the (CˆS)-cycloaurated complexes studied in this work.

subunit was kindly provided by Dr. G. Nemerow [29]. The cell lines were propagated in Dulbecco's modified Eagle's medium (DMEM; Life Technologies/Thermo Fisher Scientific) supplemented as previously reported [30]. The HAdV5-GFP used in this study was a replication-defective HAdV containing a green fluorescent protein (eGFP) reporter gene cassette, under the regulation of a CMV promoter in place of the E1/E3 regions [31]. An HAdV-RFP virus expressing the red fluorescent protein (RFP) gene under the regulation of the HAdV major late promoter was kindly provided by Dr. R. Parks (Ottawa Hospital Research Institute, Canada) [32].

2.2. Synthesis of (CˆS)-cycloaurated complexes

(CˆS)-cycloaurate complexes were prepared as previously described. Briefly, the **Au(dpta)Cl_2** complex (dpta: *o*-*N*,*N*-diisopropyl-*P*,*P*-diphenylphosphinothioic amide) was synthesized via tin(IV)-gold(III) transmetalation from the corresponding chlorodimethylstannyl derivative, as previously reported [27]. **Au(dpta)(mrdtc)** and **Au(dpta)(dedtc)** complexes (mrdtc: morpholine-4-dithiocarbamate; dedtc: diethyl dithiocarbamate) were synthesized via an overnight reaction of the **Au(dpta)Cl_2** complex with the corresponding dithiocarbamate salt in methanol, followed by the addition of aqueous potassium hexafluorophosphate [28]. Similarly, the, **Au(bpta)(dedtc)** complex (bpta = *ortho*-bis(*N*,*N*-diethyl)-*P*-phenylphosphonothioic amide; dmdtc = dimethyl dithiocarbamate) was synthesized from the corresponding **Au(bpta)Cl_2** complex [33]. See the Supporting Information for the structural characterization.

2.3. Cytotoxicity assay

The cytotoxicity of the assessed compounds was evaluated using an AlamarBlue cell viability assay (Invitrogen, Waltham, USA). Briefly, A549 cells (1×10^4 cells/well) were seeded in 96-well plates. Compounds were serially diluted from 200 to 0 μM in 100 μL of complete DMEM in triplicate. The cells were then incubated for 48 h at 37 °C in a 5% CO_2 atmosphere. Following incubation, the AlamarBlue viability reagent (Invitrogen, Waltham, USA) was added to the cells (1/10th), with subsequent incubation for a further 3 h. The half-maximal cytotoxic concentration (CC_{50}) was determined using the statistical package GraphPad Prism, and the selectivity index (SI) values were calculated as the ratio of CC_{50} to IC_{50}, with IC_{50} defined as the concentration of a compound that inhibited HAdV infection by 50%.

2.4. Plaque assay

The anti-HAdV activity of the (SˆC)-cycloaurated complexes was assessed at a low multiplicity of infection (MOI: 0.06 vp/cell) using concentrations ranging from 10 to 0.3125 μM. For each of the assessed treatments, 293β5 cells were seeded in duplicate in six-well plates at a density of 1×10^6 cells/well. After 24 h, the cells were infected with HAdV5-GFP and rocked for 2 h at 37 °C. Thereafter, the inoculum was replaced with 2 mL/well of equal parts 1.6% (water/vol) agar (VWR International Eurolab S.L.) and 2 × Minimum essential Eagle's medium (EMEM; BioWhittaker), as previously described [30]. At 3-day intervals, the cells were overlaid again with 1 mL/well of agar, EMEM, and the compound mixtures. After 7 days at 37 °C in a 5% CO_2 atmosphere, virus plaques, as measured by HAdV-mediated GFP expression, were scanned using a Typhoon Fla 9000 scanner (GE Healthcare Life Sciences) and quantified using ImageJ software [34]. IC_{50} values were determined using GraphPad Prism software.

2.5. Virus yield reduction assay

The capacity of (CˆS)-cycloaurated complexes to reduce the production of viral progeny was evaluated using a yield reduction assay. Briefly, A549 cells were seeded in 24-well plates at 1.5×10^5 cells/well, and on reaching 90% confluence, were infected with wild-type HAdV5 (100 vp/cell) in the presence of **Au(dpta)(mrdtc)** at 2-fold the IC_{50} concentration and **Au(dpta)Cl_2**, **Au(bpta)(dmdtc),** and **Au(dpta)(dedtc)** at 10-fold the IC_{50} concentration, or the same volume of dimethylsulphoxide (DMSO) used as a positive control. After 48 h at 37 °C in a 5% CO_2 atmosphere, the cells were harvested and subjected to three freeze-thaw cycles. The IC_{50} value for each treatment was calculated using an end-point dilution method [40].

2.6. Time of addition assay

The time of addition activity of the (CˆS)-cycloaurated complexes was evaluated at −60 min and 0, 2, 6, 12, and 24 h, based on a time-curve assay using Corning black wall, clear bottom 96-well plates containing A549 cells (3×10^4 cells/well) infected with HAdV-RFP (2000 vp/cell) in the presence of **Au(dpta)(mrdtc)** at 2-fold the IC_{50} concentration and AuC1, **Au(bpta)(dedtc,** and **Au(dpta)(dedtc)** at 10-fold the IC_{50} concentration, or the same volume of DMSO (positive control). For the −60-min treatment, HAdV-RFP was incubated with the selected compounds on ice for 1 h and then incubated with cells for a further 1 h. Thereafter, the inoculum was removed and replaced with complete DMEM. For the remainder of the treatments, cells were infected for 1 h at 37 °C and the respective compounds were added at the indicated times. A standard infection curve was generated in parallel by infecting cells in the absence of compounds using 2-fold serial dilutions of the virus from an MOI of 2000 vp/cell, thereby enabling an extrapolation of the RFP fluorescence obtained for each compound and the corresponding MOI. Plates were scanned using a Typhoon Fla 9000 scanner (GE Healthcare Life Sciences) and quantified using ImageQuant TL software (GE Healthcare Life Sciences).

2.7. Real-time PCR quantification of HAdV DNA

A549 cells were seeded in 24-well plates (150,000 cells/well) and having reached 90% confluency, were infected with wild-type HAdV5 (100 vp/cell). The infected cells were thereafter incubated in triplicate in complete DMEM for 16 h at 37 °C and 5% CO_2 in the presence of **Au(dpta)(mrdtc)** at 1- and 2-fold the IC_{50} concentration, **Au(dpta)Cl_2**, **Au(bpta)(dedtc),** and **Au(dpta)(dedtc)** at 2- and 10-fold the IC_{50} concentrations, or the same volume of DMSO (positive control). Following incubation, DNA was purified from cell lysates using an E.Z.N.A Tissue DNA Kit (Omega Biotek, Norcross, GA, USA) in accordance with the manufacturer's instructions. The TaqMan primers, probes, and PCR conditions used in this study have been described previously [30].

As an internal control for PCR amplification, we used the human glyceraldehyde-3-phosphate dehydrogenase (*GAPDH*) gene. The oligonucleotide sequences for *GAPDH* amplification and the PCR conditions used have been reported previously reported [35]. For quantification, HAdV hexon gene fragments and *GAPDH* were used to generate a parallel standard curve for each experiment. All assays were performed using a LightCycler 96 System thermal cycler (Roche).

2.8. Nuclear-associated HAdV genomes

Nuclear delivery of the HAdV genomes was assessed by real-time PCR following nuclear isolation from infected cells. Briefly, A549 cells seeded in six-well plates at 1×10^6 cells/well were infected with wild-type HAdV5 at an MOI of 2000 vp/cell in complete DMEM containing the assessed compounds at 10-fold the IC_{50} concentrations or the same volume of DMSO (positive control). The infected cells were incubated for 45 min at 37 °C in a 5% CO_2 atmosphere, following which they were harvested, resuspended in 500 μL of 1 × hypotonic buffer (20 mM Tris-HCl, pH 7.4, 10 mM NaCl, 3 mM $MgCl_2$), and incubated on ice for 20 min. Thereafter, following the addition of 25 μL of NP-40 detergent, the cell suspensions were centrifuged for 10 min at 835×*g* and 4 °C to separate the nuclear (pellet) and cytoplasmic (supernatant) fractions. Finally, DNA was isolated from the nuclear fraction using an E.Z.N.A Tissue DNA Kit (Omega Biotek, Norcross, GA, USA) [30].

2.9. Synergistic activity

Compounds along with CDV at concentrations ranging from 2- to 0.125-fold the corresponding IC_{50} values were assessed using a single plaque assay. Briefly, 293β5 cells were seeded in plates at 1×10^6 cells/well and infected with HAdV-GFP at a low MOI (0.06 vp/cell) for 2 h at 37 °C. Thereafter, the inoculum was removed and the cells were carefully overlaid with equal parts of agar and EMEM

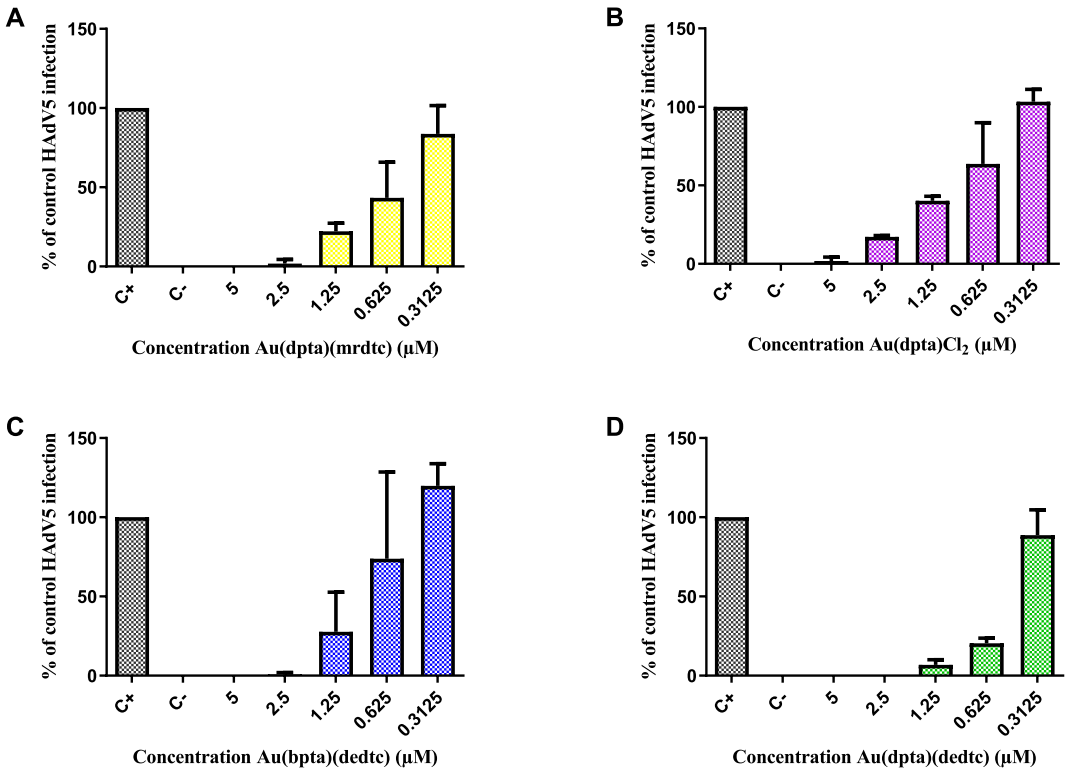

Fig. 2. Inhibitory activity of **A) Au(dpta)Cl_2, B) Au(dpta)(mrdtc), C) Au(bpta)(dmdtc)** and **D) Au(dpta)(dedtc)**. Dose-dependent activity against HAdV5 in a plaque assay at low MOI (0.06 vp/cell). Results represent means ± SD of triplicate samples from independent experiments.

containing the assessed drugs. At 3-day intervals, the cells were overlaid again with 1 mL/well of a mixture of agar, EMEM, and compounds. Following a 7-day incubation at 37 °C in a 5% CO_2 atmosphere, viral plaques were analysed using CalcuSyn software to determine the associated combination index [36].

2.10. Real-time PCR quantification of HCMV DNA

To assess the anti-HCMV (MOI of 0.05 vp/cell) activity of the synthesized (CˆS)-cycloaurate complexes, we used HFF cells seeded at a density of 8.3×10^4 cells/well in 24-well plates. The assay was performed in triplicate in the presence of compounds at 1-, 2-, and 5-fold the established HAdV IC_{50} values or the same volume of DMSO, and the cells were incubated for 72 h at 37 °C in a 5% CO_2 atmosphere. Thereafter, HCMV DNA was purified from the cell lysates using an E.Z.N.A Tissue DNA Kit (Omega Biotek, Norcross, GA, USA). The primers, reaction mixtures, and protocols we used for real-time PCR have been reported previously [37].

2.11. Statistical analyses

One-way ANOVA (Dunnett's method) was used to evaluate the differences in infection among the assayed compounds using the GraphPad Prism 6 software. A p value < 0.05 was considered to be indicative of a statistical significance (**P < 0.01, ***P < 0.001, ****P < 0.0001).

3. Results

3.1. Anti-HAdV activity

The four (CˆS)-cycloaurated complexes synthesized in this study were evaluated using a plaque assay to determine their inhibitory activity against HAdV. All four compounds exhibited a dose-dependent anti-HAdV activity (Fig. 2), with 100% inhibition being observed for **Au(dpta)(mrdtc)**, **Au(bpta)(dedtc),** and **Au(dpta)(dedtc),** and over 95% inhibition for **Au(dpta)Cl_2** when applied at a concentration of 5 μM. In a yield reduction assay, the compounds' capacity to reduce viral replication was evaluated, and revealing reductions ranging from 250-fold for **Au(dpta)(mrdtc)** at 2-fold the IC_{50} concentration to a 30×10^3-fold reduction at 10-fold the IC_{50} concentration for **Au(dpta)Cl_2** (Table 1). For all four of the assessed complexes, the respective cytotoxic concentrations were found to be higher than the corresponding IC_{50} values, with SI values ranging from 6.65 for **Au(dpta)(mrdtc)** to 22.76 for **Au(dpta)(dedtc)**. The IC_{50}, $CC_{50,}$ SI, and yield reduction values obtained for the four complexes are summarized in Table 1.

3.2. Time of addition assay

Having initially established the anti-HAdV activity of the assessed complexes, we subsequently sought to determine the stage at which these complexes disrupt the replicative cycle of HAdV. We also measured the effect of addition time on the efficacy of the compounds (Fig. 3). All derivatives exhibited a time-dependent reduction in inhibitory activity. When added at the beginning of a 60-min incubation at 4 °C (−60 min), **Au(dpta)Cl_2** and **Au(bpta)(dedtc)** inhibited 100% of HAdV infection, whereas the **Au(bpta)(dedtc)** complex induced 100% inhibition at 0 and 6 h. For virus exposed to **Au(dpta)(mrdtc)** and **Au(dpta)(dedtc),** the 50%–70% levels of inhibition detected at 60 min remained unchanged until the 12-h time-point, at which it declined to 15%–50%. However, among the four assessed complexes, only **Au(bpta)(dedtc)** was found to cause >50% inhibition after 24 h.

3.3. DNA-quantification and nuclear association

We initially evaluated the capacity of the synthesized cycloaurated complexes to block the HAdV DNA replication process using a real-time PCR assay in a single round of infection in the presence or absence of the four complexes at different concentrations. Any of the four complexes showed the ability to inhibit the DNA replication process (Fig. 4). Additionally, to confirm whether any of these complexes interfered with a step between HAdV entry and HAdV DNA import into the nucleus, we examined the capacity of the HAdV genome to gain access to the cell nucleus. As shown in Fig. 5, compared with DMSO control, treatment with any of these four complexes had no significant effect on the number of HAdV genomes that reached the nucleus. This result indicate that none of these complexes interfered with the early stages of HAdV infection.

Table 1
$IC_{50,}$ $CC_{50,}$ SI and yield reduction values for **Au(dpta)Cl_2**, **Au(dpta)(mrdtc)**, **Au(bpta)(drdtc)** and **Au(dpta)(dedtc) against HAdV5. The results represent means ± SD of triplicate samples**.

Compound	IC_{50} (μM)	CC_{50} (μM)	SI	Virus Yield Fold-Reduction*
Au(dpta)(mrdtc)	0.60 ± 0.18	3.99 ± 0.7	6.65	250 ± 218.16
Au(dpta)Cl_2	0.93 ± 0.30	17.97 ± 2.54	19.32	26800 ± 5083
Au(bpta)(dedtc)	0.87 ± 0.48	13.68 ± 1.55	15.72	31899 ± 0
Au(dpta)(dedtc)	0.43 ± 0.04	9.79 ± 1.96	22.76	13200 ± 8525

Compound tested at 2-fold of Au(dpta)(mrdtc) and 10-fold of Au(dpta)Cl_2, Au(bpta)(dedtc) and Au(dpta)(dedtc).

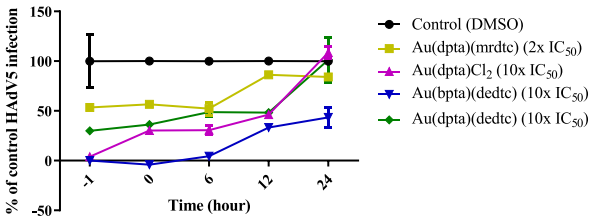

Fig. 3. Time of addition assay. Effect of **Au(dpta)Cl_2**, **Au(dpta)(mrdtc)**, **Au(bpta)(dedtc)** and **Au(dpta)(dedtc)** on HAdV infection at different points at 2 and 10-fold the IC_{50} concentration obtained in the plaque assay for each of them. The DMSO control is a negative control with cells infected at the same MOI and treated with DMSO at the same time points but in the absence of compounds. Results represent means ± SD of triplicate samples.

3.4. Combined activity of cycloaurated complexes and CDV

Correlation coefficients of the median-effect plot between 0.91 and 0.99 were reported, indicating good conformity to the mass-action law (Table 2). The combination treatment with CDV and **Au(dpta)(mrdtc)** exhibited antagonistic activity at effective doses, including ED_{50}, ED_{75}, and ED_{90}. In contrast, the effect of the combination of CDV with **Au(dpta)Cl_2** or **Au(bpta)(dedtc)** was almost additive at ED_{50}, ED_{75}, and ED_{90}. Comparatively, the combination of CDV and **Au(dpta)(dedtc)** was the most effective, showing a slight synergistic effect at the three assessed effective doses.

3.5. Anti-HCMV activity

To assess the potential broad-spectrum activity of the four complexes, we examined their activity against HCMV. Exposure of HCMV to **Au(dpta)(mrdtc)**, **Au(dpta)Cl_2**, **Au(bpta)(dedtc),** and **Au(dpta)(dedtc)** at the HAdV IC_{50} concentration resulted in its inhibitions of 58%, 67% and 46%, respectively, whereas **Au(dpta)(dedtc)** exhibited a 90% inhibition. When administered at 2-fold the HAdV IC_{50} concentration, the four complexes exhibited inhibition levels surpassing 80%. Similarly, at 5-fold the HAdV IC_{50} concentration (Fig. 6), inhibition levels of 96%, 99%, and 97% were obtained for viruses treated with **Au(dpta)Cl_2**, **Au(bpta)(dedtc),** and **Au(dpta)(dedtc)**, respectively.

4. Discussion

In this study, we aimed to evaluate the antiviral activity of four (CˆS)-cycloaurate complexes against HAdV and HCMV, and characterize their potential mechanisms of action. Our results revealed that all four complexes inhibited these two viruses at sub-micromolar concentrations, with IC_{50} values against HAdV ranging from 0.43 to 0.93 μM. Similarly, Gil-Moles et al., assessed the efficacy of auranofin and five gold organometallics in inhibiting two SARS-CoV-2 targets, spike-ACE2 interaction and papain-like protease (PLpro). They obtained IC_{50} values ranging from 16.2 to 25 μM and 0.75 to >100 μM, respectively [15]. Concerning the cytotoxicity of the four (CˆS)-cycloaurate complexes, we obtained values ranging from 3.99 μM for **Au(dpta)(mrdtc)** to 17.97 μM for

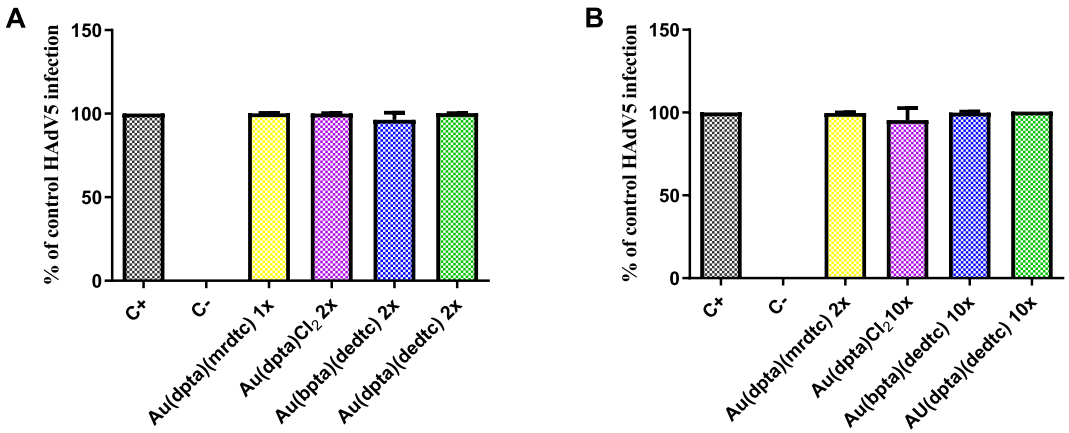

Fig. 4. Impact of **Au(dpta)Cl_2**, **Au(dpta)(mrdtc)**, **Au(bpta)(dedtc)** and **Au(dpta)(dedtc)** on HAdV DNA replication. **A)** Impact of 1-fold of Au(dpta)(mrdtc) and 2-fold of Au(dpta)Cl_2, Au(bpta)(dedtc) and Au(dpta)(dedtc) HAdV IC_{50} concentration. **B)** Impact of 2-fold of Au(dpta)(mrdtc) and 10-fold of Au(dpta)Cl_2, Au(bpta)(dedtc) and Au(dpta)(dedtc) HAdV IC_{50} concentration. The negative control (−) is non-infected cells, while the positive control (+) is cells infected at the same MOI but in absence of compound. Data are presented as the mean ± SD from triplicate assays. No statistical significance differences were observed.

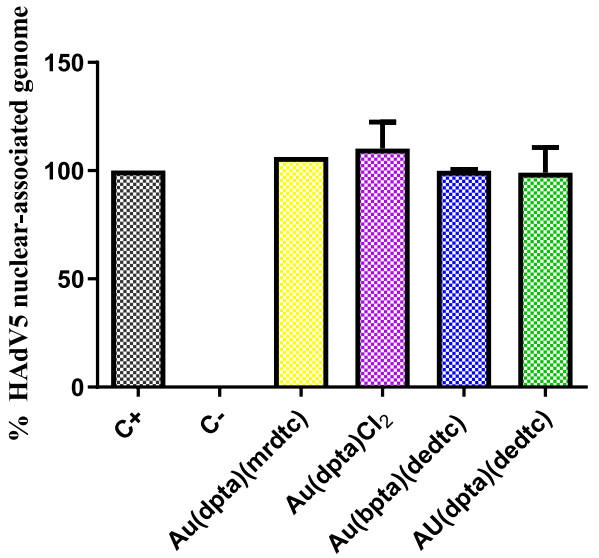

Fig. 5. Impact of **Au(dpta)Cl_2**, **Au(dpta)(mrdtc)**, **Au(bpta)(dedtc)** and **Au(dpta)(dedtc)** on HAdV accessibility to the nucleus cell. Percentage of nuclear-associated HAdV genome of **Au(dpta)Cl_2**, **Au(dpta)(mrdtc)**, **Au(bpta)(dedtc)** and **Au(dpta)(dedtc)** at 10-fold HAdV IC_{50} concentration after 45 min of incubation. No statistical significance differences were observed.

Table 2
CalcuSyn results for the different combinations of **Au(dpta)Cl_2**, **Au(dpta)(mrdtc)**, **Au(bpta)(dedtc)** and **Au(dpta)(dedtc)** with CDV.

Ratio combination	Compound	Simple IC_{50} (μM)	In combination IC_{50} (μM)	Combinatión index value			
				ED50	ED75	ED90	r
CDV + Au(dpta)(mrdtc) (40:1)	CDV	24 ± 5.9	14.33 ± 0.46	1.58816	1.54486	1.50429	0.94857
	Au(dpta)(mrdtc)	0.6 ± 0.18	0.36 ± 0.01				
CDV + Au(dpta)Cl_2 (26:1)	CDV	24 ± 5.9	17.43 ± 3.37	1.00232	0.99297	0.98495	0.91220
	Au(dpta)Cl_2	0.93 ± 0.30	0.68 ± 0.13				
CDV + Au(bpta)(dedtc) (28:1)	CDV	24 ± 5.9	14.37 ± 1.39	0.99440	1.04387	1.09587	0.97667
	Au(bpta)(dmdtc)	0.87 ± 0.48	0.52 ± 0.05				
CDV + Au(dpta)(dedtc) (56:1)	CDV	24 ± 5.9	12.08 ± 1.23	0.89841	0.89232	0.88675	0.98942
	Au(dpta)(dedtc)	0.43 ± 0.04	0.22 ± 0.02				

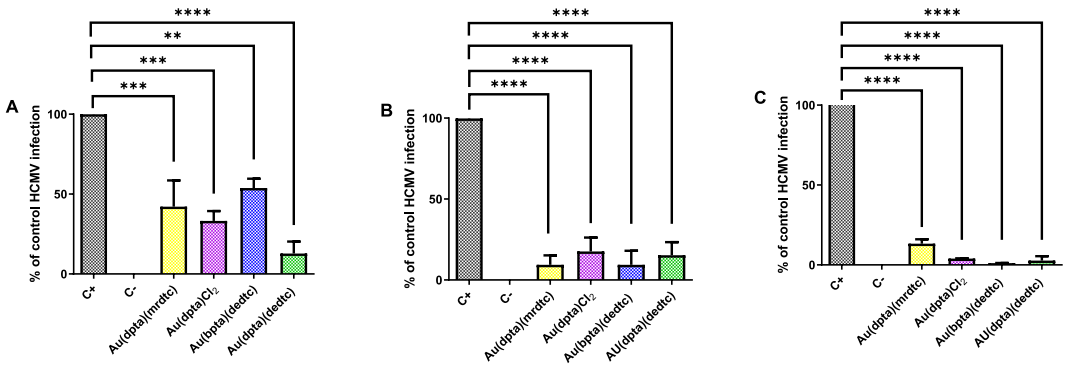

Fig. 6. Effect of **Au(dpta)Cl_2**, **Au(dpta)(mrdtc)**, **Au(bpta)(dedtc)** and **Au(dpta)(dedtc)** on HCMV DNA replication at **A)** 1-fold, **B)** 2-fold and **C)** 5-fold HAdV IC_{50} concentration. The negative control (−) is non-infected cells, while the positive control (+) is cells infected at the same MOI but in absence of compound. Data are presented as the mean ± SD from triplicate assays. (**$P < 0.01$, ***$P < 0.001$, ****$P < 0.0001$).

Au(dpta)Cl_2. These values are consistent with those reported by Aires et al. for four Au(I) derivatives, In their study, the highest non-cytotoxic concentration assessed was 10 μM, and only two of the derivatives maintained a CHIKV inhibition >90% [17]. Although the **Au(dpta)(dedtc)** complex assessed in the present study did not show the lowest CC_{50} value, we found that its high antiviral activity resulted in a better IS.

The replication cycle of HAdV consists of early and late phases. The early phase spans from virus binding to cellular receptors to the release of its genetic material into the host cell nucleus, whereas the late phase involves the expression of HAdV early proteins, replication of HAdV DNA, translation of late viral mRNAs, and the assembly and release of new viral particles [38,39]. Therefore, we conducted mechanistic studies to identify which of these two stages is targeted by the four assessed compounds. Previous reports indicated that HAdV particles reach the nuclear membrane within 1 h of cellular infection, and viral DNA and proteins can be detected within the nucleus 1 and 2 h later [38]. The early phase of HAdV replication extends to 6–8 h, whereas the late phase is completed more rapidly, yielding virus after an additional 4–6 h. To determine whether the assessed compounds act during the early or late stages, we initially examined the activity of the four complexes against HAdV at different time points. Subsequently, we found that when added between 1 h before and 6 h after infection, **Au(bpta)(dedtc)** exhibited 100% inhibition of HAdV-mediated GFP expression. This result indicate that **Au(bpta)(dedtc)** targets the HAdV during early phase of replication. Similarly, pre-incubation with the **Au(bpta)Cl_2** complex contributed to a 100% inhibition of HAdV infection. The observed reduction in this inhibitory activity to 30% at 0 h and 6 h after infection suggests that the target of this compound is disrupted during the early phase of infection and involves a direct interaction with the viral particles. Among the assessed complexes, **Au(dpta)(dedtc)** demonstrated the most pronounced inhibition of the HAdV transgene expression when pre-incubated with the virus and at 0 and 6 h post-infection. Its activity sharply declined when added after 12 h, consistent with a target late in the HAdV replicative cycle. Compared with the activity of the other three complexes, that of **Au(dpta)(mrdtc)** was somewhat weaker, causing a 50% inhibition of HAdV transgene expression from pre-incubation with the virus to its addition at the 6-h time point, and thereafter losing its inhibitory activity.

To confirm these results, we evaluated the effects of these complexes on the capacity of HAdV viral particles to enter the nucleus, and accordingly established that none of the complexes block nuclear access. This result implies that they do not interfere with the early stages of HAdV infection. Additionally, we assessed the efficacies of these complexes in inhibiting the HAdV DNA replication process. This analysis indicated a reduction in the efficiency of replication and yield of the HAdV genomes in a 6-h assay. None of the assayed complexes appeared to reduce the DNA replication efficiency of the virus over the course of the 6-h assay. Moreover, consistent with the data obtained from our time-of-addition assay, all four of the assessed complexes were characterized by a reduced inhibitory activity after 6 h.

Given that CDV is a non-specific option for treating HadV, albeit with variable performance regarding efficacy and safety, we evaluated the effects of combined treatments with CDV and each of the four synthesized (CˆS)-cycloaurate complexes to assess their potential synergistic activity. The combination of CDV and **Au(dpta)(dedtc)**, the complex with highest SI value, was found to be most effective in this respect. Finally, to determine whether these complexes have broad-spectrum antiviral activity, their inhibitory activity against HCMV, another DNA virus, was assessed. Notably, all four complexes were found to almost completely block HCMV DNA replication in a 72-h assay, with **Au(dpta)(dedtc)** characterized by the highest inhibitory activity.

5. Conclusions

Collectively, the findings of our study revealed that each of the four assessed (CˆS)-cycloaurated complexes exhibited potent antiviral activity against HAdV and HCMV at sub-micromolar concentrations, and they appeared to target the late stages of the HAdV replicative cycle after DNA replication. Among the assessed compounds, **Au(dpta)(dedtc)** was identified as having the best SI and highest anti-HCMV activity. Thus, this (CˆS)-cycloaurated complex could be considered a promising candidate for the development and evaluation of a novel series of derivatives with the aim of optimizing antiviral activities and cytotoxicity profiles until achieve to a lead compound that could enter in preclinical stages.

Data availability statement

Data associated with the study have not been deposited into a publicly available repository because of the data are included in the manuscript and/or in the supplementary file. The previous data that support the findings of this study are available from the corresponding authors (FLO/SMS) upon reasonable request.

CRediT authorship contribution statement

María Balsera-Manzanero: Writing – original draft, Methodology, Formal analysis. **Raquel G. Soengas:** Writing – review & editing, Investigation, Conceptualization. **Marta Carretero-Ledesma:** Writing – review & editing, Writing – original draft, Methodology, Formal analysis. **Carlos Ratia:** Investigation. **M. José Iglesias:** Investigation. **Jerónimo Pachón:** Writing – review & editing, Resources, Investigation. **Fernando López Ortiz:** Writing – review & editing, Investigation, Conceptualization. **Elisa Cordero:** Investigation, Conceptualization. **Sara M. Soto:** Writing – review & editing, Supervision, Funding acquisition, Conceptualization. **Javier Sánchez Céspedes:** Writing – review & editing, Writing – original draft, Validation, Resources, Funding acquisition, Formal analysis, Conceptualization.

Declaration of competing interest

The authors declare that they have no known competing financial interests or personal relationships that could have appeared to influence the work reported in this paper.

Acknowledgements

This work was partially supported by the Instituto de Salud Carlos III, Ministerio de Ciencia e Innovación, co-funded by the European Development Regional Fund Proyectos de Investigación en Salud (PI18/01191, PI19/00478), and Proyectos de Desarrollo Tecnológico en Salud (DTS20/00010, DTS21/00004). JSC (CB21/13/00006) and S.M.S. (CB21/13/00081) also received support from the CIBER de Enfermedades Infecciosas (CIBERINFEC), Instituto de Salud Carlos III, Ministerio de Ciencia e Innovación, co-funded by the European Development Regional Fund. J.S.C is supported by the program "Nicolás Monardes" (C-0059-2018) Servicio Andaluz de Salud, Junta de Andalucía. ISGlobal is a CERCA center from the Generalitat of Catalunya and a Severo Ochoa Center (Spanish Ministry of Science, Innovations, and Universities).

Appendix A. Supplementary data

Supplementary data to this article can be found online at https://doi.org/10.1016/j.heliyon.2024.e27601.

References

[1] K.M. MacNeil, et al., Adenoviruses in medicine: innocuous pathogen, predator, or partner, Trends Mol. Med. 29 (1) (2023) 4–19.
[2] M.J. Dodge, et al., Emerging antiviral therapeutics for human adenovirus infection: recent developments and novel strategies, Antivir. Res. 188 (2021) 105034.
[3] B. Saha, R.J. Parks, Recent advances in novel antiviral therapies against human adenovirus, Microorganisms 8 (9) (2020).
[4] J.P.S. Begum, et al., Emergence of monkeypox: a worldwide public health crisis, Hum. Cell 36 (3) (2023) 877–893.
[5] M. Moshirfar, et al., The impact of antiviral resistance on herpetic keratitis, Eye Contact Lens 49 (3) (2023) 127–134.
[6] M.S. Grimley, et al., Preliminary results from the advise study evaluating brincidofovir (CMX001, BCV) for the treatment of disseminated and high-risk adenovirus (AdV) infection, Biol. Blood Marrow Transplant. 21 (2) (2015) 108–109.
[7] G. Chittick, et al., Short-term clinical safety profile of brincidofovir: a favorable benefit–risk proposition in the treatment of smallpox, Antivir. Res. 143 (2017) 269–277.
[8] R. Mehrotra, S.N. Shukla, P. Gaur, Metallo-antiviral aspirants: answer to the upcoming virus outbreak, Eur J Med Chem Rep 8 (2023) 100104.
[9] R.E.F. de Paiva, et al., What is holding back the development of antiviral metallodrugs? A literature overview and implications for SARS-CoV-2 therapeutics and future viral outbreaks, Dalton Trans. 49 (45) (2020) 16004–16033.
[10] Y. Liu, et al., Repurposing of the gold drug auranofin and a review of its derivatives as antibacterial therapeutics, Drug Discov. Today 27 (7) (2022) 1961–1973.
[11] C.A.M. Fonseca, Biological activity of gold compounds against viruses and parasitosis: a systematic review, BioChemistry (Rajkot, India) 2 (2022) 145–159.
[12] B.C. Dominelli, D.G. J, F.E. Kühn, Medicinal applications of gold(I/III)-Based complexes bearing N-heterocyclic carbene and phosphine ligands, J. Organomet. Chem. 866 (2018) 153–164.
[13] J.R. Stenger-Smith, P.K. Mascharak, Gold drugs with Au(PPh(3))(+) moiety: advantages and medicinal applications, ChemMedChem 15 (22) (2020) 2136–2145.
[14] A.E. Finkelstein, et al., Auranofin. New oral gold compound for treatment of rheumatoid arthritis, Ann. Rheum. Dis. 35 (3) (1976) 251–257.
[15] M. Gil-Moles, et al., Gold metallodrugs to target coronavirus proteins: inhibitory effects on the spike-ACE2 interaction and on PLpro protease activity by auranofin and gold organometallics, Chemistry 26 (66) (2020) 15140–15144.
[16] L.G. Tunes, et al., Preclinical gold complexes as oral drug candidates to treat leishmaniasis are potent trypanothione reductase inhibitors, ACS Infect. Dis. 6 (5) (2020) 1121–1139.
[17] R.L. Aires, et al., Triphenylphosphine gold(I) derivatives promote antiviral effects against the Chikungunya virus, Metallomics 14 (8) (2022).
[18] C.D. Lopes, et al., Organometallic gold(III) complex [Au(Hdamp)(L1(4))](+) (L1 = SNS-donating thiosemicarbazone) as a candidate to new formulations against Chagas disease, ACS Infect. Dis. 5 (10) (2019) 1698–1707.
[19] P.N. Fonteh, F.K. Keter, D. Meyer, New bis(thiosemicarbazonate) gold(III) complexes inhibit HIV replication at cytostatic concentrations: potential for incorporation into virostatic cocktails, J. Inorg. Biochem. 105 (9) (2011) 1173–1180.
[20] A.A.N.A.M. Najim, M.T. Abdulalah, Synthesis and in vitro anti-HIV activity of some new schiff base ligands derived from 5-Amino-4-phenyl-4H-1,2,4-triazole-3-thiol and their metal complexes, Phosphorus, Sulfur, Silicon Relat. Elem. 184 (11) (2009) 2891–2901.
[21] P.N. Fonteh, et al., Tetra-chloro-(bis-(3,5-dimethylpyrazolyl)methane)gold(III) chloride: an HIV-1 reverse transcriptase and protease inhibitor, J. Inorg. Biochem. 103 (2) (2009) 190–194.
[22] M. Mphahlele, et al., Modification of HIV-1 reverse transcriptase and integrase activity by gold(III) complexes in direct biochemical assays, Bioorg. Med. Chem. 20 (1) (2012) 401–407.
[23] R.W. Sun, et al., In vitro inhibition of human immunodeficiency virus type-1 (HIV-1) reverse transcriptase by gold(III) porphyrins, Chembiochem 5 (9) (2004) 1293–1298.
[24] M. Gil-Moles, et al., Metallodrug profiling against SARS-CoV-2 target proteins identifies highly potent inhibitors of the S/ACE2 interaction and the papain-like protease PL(pro), Chemistry 27 (71) (2021) 17928–17940.
[25] G. Moreno-Alcantar, P. Picchetti, A. Casini, Gold complexes in anticancer therapy: from new design principles to particle-based delivery systems, Angew Chem. Int. Ed. Engl. 62 (22) (2023) 202218000.
[26] L.A. Pazderski, P.A. Au III, Cyclometallated compounds with 2-arylpyridines and their derivatives or analogues: 34 Years (1989–2022) of NMR and single crystal X-ray studies, INORGA 11 (3) (2023).
[27] C. Ratia, et al., A C(wedge)S-cyclometallated gold(III) complex as a novel antibacterial candidate against drug-resistant bacteria, Front. Microbiol. 13 (2022) 815622.
[28] C. Ratia, et al., Gold(III) complexes activity against multidrug-resistant bacteria of veterinary significance, Antibiotics 11 (12) (2022).
[29] E.K. Nguyen, G.R. Nemerow, J.G. Smith, Direct evidence from single-cell analysis that human alpha-defensins block adenovirus uncoating to neutralize infection, J. Virol. 84 (8) (2010) 4041–4049.
[30] S. Mazzotta, et al., Serinol-based benzoic acid esters as new scaffolds for the development of adenovirus infection inhibitors: design, synthesis, and in vitro biological evaluation, ACS Infect. Dis. 7 (6) (2021) 1433–1444.
[31] R.R. Nepomuceno, L. Pache, G.R. Nemerow, Enhancement of gene transfer to human myeloid cells by adenovirus-fiber complexes, Mol. Ther. 15 (3) (2007) 571–578.
[32] B. Saha, et al., Development of a novel screening platform for the identification of small molecule inhibitors of human adenovirus, Virology 538 (2019) 24–34.
[33] K.J. Kilpin, W. Henderson, B.K. Nicholson, Cycloaurated triphenylphosphine-sulfide and -selenide, Dalton Trans. 39 (7) (2010) 1855–1864.
[34] C.A. Schneider, W.S. Rasband, K.W. Eliceiri, NIH Image to ImageJ: 25 years of image analysis, Nat. Methods 9 (7) (2012) 671–675.
[35] A.A. Rivera, et al., Mode of transgene expression after fusion to early or late viral genes of a conditionally replicating adenovirus via an optimized internal ribosome entry site in vitro and in vivo, Virology 320 (1) (2004) 121–134.

[36] J. Xu, et al., Discovery of novel substituted N-(4-Amino-2-chlorophenyl)-5-chloro-2-hydroxybenzamide analogues as potent human adenovirus inhibitors, J. Med. Chem. 63 (21) (2020) 12830–12852.
[37] S. Mazzotta, et al., Optimization of piperazine-derived ureas privileged structures for effective antiadenovirus agents, Eur. J. Med. Chem. 185 (2020) 111840.
[38] W.C. Russell, Update on adenovirus and its vectors, J. Gen. Virol. 81 (Pt 11) (2000) 2573–2604.
[39] Y. Zhang, D. Feigenblum, R.J. Schneider, A late adenovirus factor induces eIF-4E dephosphorylation and inhibition of cell protein synthesis, J. Virol. 68 (11) (1994) 7040–7050.
[40] L.J. Reed, H. Muench, A Simple Method ofEstimating Fifty Per Cent Endpoints, Am. J. Epidemiol. 27 (3) (1938) 493–497.